Subnanosecond lifetime measurement for the T=0, 31+ state of odd-odd N = Z 58Cu

Subnanosecond lifetime measurement for the $T = 0$, 3_1^+ state of odd-odd N = Z ^{58}Cu

A. Costin, N. Pietralla, T. Koike, C. Vaman, T. Ahn, and G. Rainovski*

Nuclear Structure Laboratory, SUNY at Stony Brook, Stony Brook, New York 11794-3800, USA

(Received 18 July 2005; published 16 November 2005)

We have measured the lifetime of the $T = 0$, $J^\pi = 3_1^+$ state of ^{58}Cu at 444 keV. The excited states in ^{58}Cu were populated with the ^{58}Ni$(p, n\gamma)$ reaction at the SUNY at Stony Brook TANDEM-LINAC facility. A lifetime $\tau = 0.468 \pm 0.085$ ns was found with the delayed γ-radiofrequency coincidence method with respect to the pulsed LINAC beam. It corresponds to an isoscalar $E2$ transition strength of 7.6 ± 1.4 W.u. to the $T = 0$, $J^\pi = 1_1^+$ ground state. The result agrees with the interpretation of the 3_1^+ state as a collective quadrupole excitation of the 1_1^+ ground state of ^{58}Cu.

I. INTRODUCTION

Nuclear forces tend to energetically favor states with the lowest isospin quantum number. Nuclear states with isospin greater than the lowest number are typically high in energy or even unbound in most nuclei. The only exceptions to this rule are the odd-odd N = Z nuclei. The energy difference between the lowest energy levels with the lowest isospin (here $T = 0$) and those with the next higher isospin (here $T = 1$) is considerably smaller in these nuclei than in all the others. This allows γ-ray spectroscopy of isovector transitions.

Low-energy states of odd-odd N = Z nuclei have recently been considered [1,2] as originating predominantly from the coupling of the unpaired proton and neutron to the even-even N = Z, $T = 0$, $J^\pi = 0^+$ core. Such shell model configurations that generalize the structure of the deuteron are called quasideuteron configurations (QDCs). The unique experimental signature of QDCs is the unusually strong $\Delta T = 1$ isovector $M1$ transitions in the case of $j = l + 1/2$ orbitals. These transitions have a noncollective single-particle nature. QDCs have been identified from the γ-ray decay pattern in the $f_{7/2}$-shell [3–5] and from the measurement of absolute $M1$ transitions strengths for $A < 56$ [1,6,7]. QDCs have been shown useful for the measurement of isospin mixing [8].

In the mass region with $A > 56$, ^{58}Cu is the first candidate for exhibiting QDC features. Indeed, the low-spin level scheme of ^{58}Cu [9] indicates a QDC structure. But starting already at an energy of 1052 keV, one can notice states that cannot be explained with the QDC scheme. Moreover, as observed in Ref. [9], the expected $(T = 1) \rightarrow (T = 0)$, $2_2^+ \rightarrow 1_1^+$ isovector $M1$ transition is hindered as a consequence of a Q-phonon selection rule which is a collective concept [10–12]. These facts indicate the necessity of an extension of the shell model calculations with the doubly magic inert ^{56}Ni core performed for ^{58}Cu [13,14] to full pf-shell calculations [15]. The large-scale shell model calculations show the importance of excitations across the N = Z = 28 shell gap already for ^{58}Cu. This statement is corroborated by the large experimental $B(E2; 2_2^+ \rightarrow 0_1^+)$ value of 9.1(3.5) W.u. between the two

lowest-lying $T = 1$ states of ^{58}Cu. Note that this $\Delta T = 0$ collective $E2$ strength has been measured so far only between states with isospin $T = 1$ which could in principle contain both isoscalar and isovector contributions to the matrix element.

Due to the outstanding importance of shell closures for the understanding of nuclear structure, in particular, for heavy nuclei along the N = Z line in the vicinity of the astrophysically important rp process [16] path, it is desirable to gather information on $\Delta T = 0$ $E2$ transition strengths between $T = 0$ states of ^{58}Cu, for testing their collectivity. In this view, our experiment investigates the degree of softness of the ^{56}Ni core by determining the $B(E2; 3_1^+ \rightarrow 1_1^+)$ value in ^{58}Cu which has pure isoscalar character.

II. EXPERIMENT

Low spin states of ^{58}Cu were populated using the ^{58}Ni$(p, n\gamma)^{58}$Cu fusion evaporation reaction at the TANDEM-LINAC facility of SUNY at Stony Brook. A 14 MeV pulsed proton beam bombarded a 1 mg/cm^2 thick ^{58}Ni target. The pulsed proton beam with a frequency of 150.4 MHz and a width of about 1.5 ns allows us to measure subnanosecond lifetimes. The detection system consisted of four Compton suppressed Ge detectors mounted horizontally with respect to the beam. Two of the Ge detectors were mounted in forward direction at an angle $\theta = 45°$ with respect to the beam axis and the other two were mounted perpendicular to the beam axis. The pulses from the Ge detectors provided the start signals for the delayed γ-radiofrequency (r.f.) coincidences [17]. Signals synchronized to the LINAC r.f. were used to stop the time-to-amplitude converter. The time difference between the start and stop signals as well as the corresponding γ-ray energy were recorded and sorted off-line into γ-time matrices. The total number of events collected during the experiment was approximately 10^8 at an average count rate of 8 kHz/detector. A sample γ-ray spectrum is presented in Fig. 1.

The purpose of the experiment is to measure the lifetime τ of the 3_1^+ isomeric state in ^{58}Cu. We use the generalized centroid shift method [17]. It consists of setting cuts on the γ-ray transitions of interest and neighboring background positions and thus creating their corresponding time distributions. An example is shown in Fig. 2. After subtracting the background
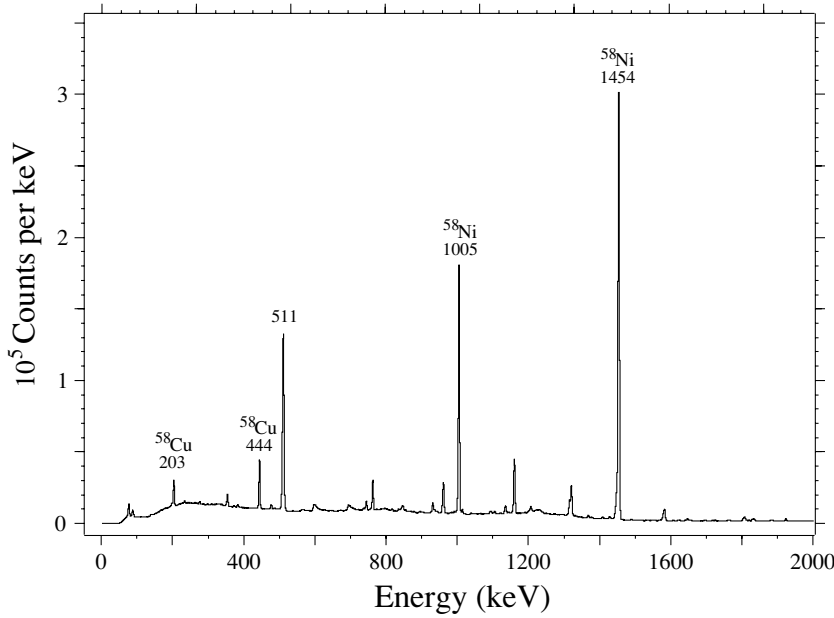

FIG. 1. The γ-ray spectrum obtained in the experiment. Prompt transitions of both ^{58}Cu and ^{58}Ni along with the delayed 444 keV and 511 keV transitions are labeled.

contributions beneath the time peak, the net time distributions are obtained. The centroids of the net time distributions of full-energy peaks and of Compton background are plotted versus γ-ray energy in the so-called centroid diagram [17]. The zero-time curve is obtained by a numerical fit of the known prompt γ-rays and their prompt Compton-background time distribution centroids. Based on its shape, the zero-time curve was fitted with several trial functions. The following fit function gives the minimum reduced χ^2:

$$f(x) = a\left(1 - be^{-cx + \frac{d}{x^2}}\right), \tag{1}$$

where a, b, c, and d are parameters determined from the fitting procedure to the data on the zero-time curve. Measurable lifetimes correspond to centroid shifts from the zero-time curve. Figure 3 clearly shows such shifts for two γ-rays,
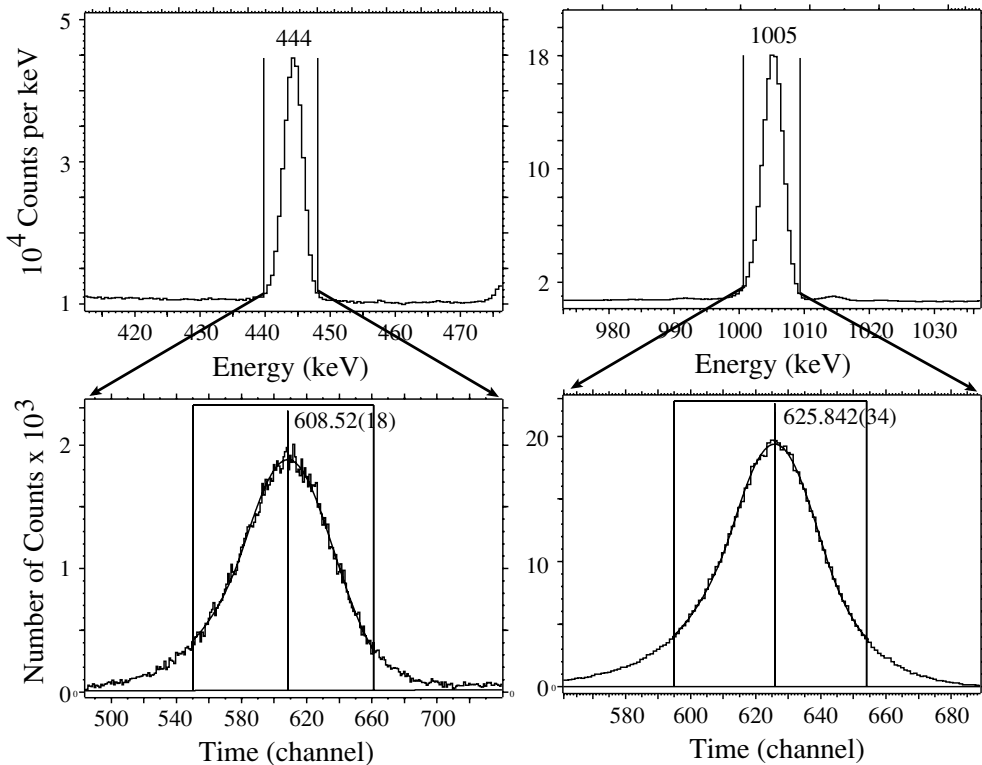

FIG. 2. Energy spectra (top) of the delayed 444 keV and prompt 1005 keV γ transitions and their corresponding time distributions (bottom).
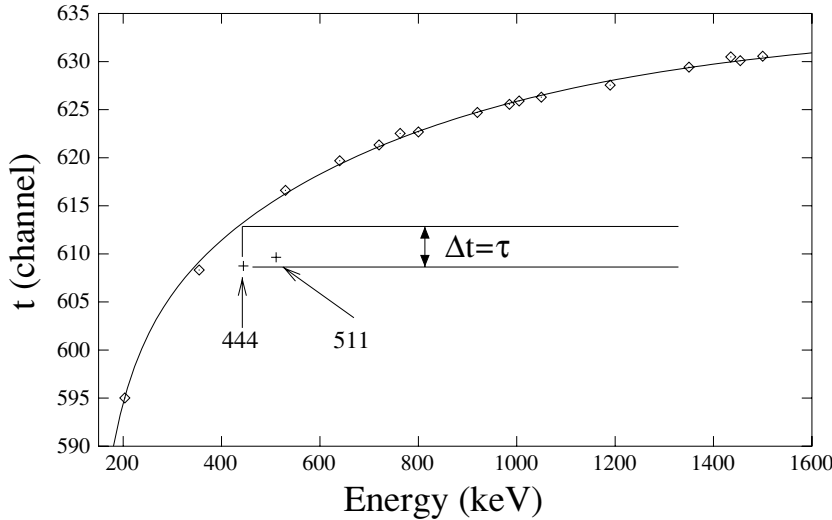
FIG. 3. Centroid diagram obtained in the ^{58}Ni$(p, n\gamma)^{58}$Cu fusion-evaporation reaction for one of the Ge detectors. Circles represent the centroids of the time distributions of the background and prompt γ transitions. The radii of the symbols correspond to the statistical errors.

the 444 keV $3_1^+ \rightarrow 1_1^+$ transition in ^{58}Cu, and the 511 keV γ-ray from electron-positron annihilation. We indeed expect the latter γ line to be delayed because the lifetime of the positron in materials amounts to hundreds of picoseconds [19]. The observed shifts from the zero-time curve amount to 4.6(10) channels for the 444 keV γ-ray and 6.0(10) chns for the 511 keV line in the example given in Fig. 3. The quoted uncertainties include statistical errors and the uncertainty of our fit for the zero-time curve.

The time calibration was accomplished by means of shifting the proton beam bunches in time relative to the oscillator signal of the LINAC by multiples of two r.f. periods $(2 \times 6.6489$ ns). The resulting profile is shown in the inset in Fig. 4. This beam-skipping procedure yields an accurate result as shown in Fig. 4, with an uncertainty in the determination of the slope of the calibration line smaller than 2 ps/ch.

The deviation from the zero-time curve measured for the time centroid of the $3_1^+ \rightarrow 1_1^+$ transition reveals a lifetime of

$$\tau = 0.468 \pm 0.085 \text{ ns}. \qquad (2)$$

This value was obtained from an average over the observed centroid shifts. It corresponds to a $B(E2; 3_1^+ \rightarrow 1_1^+)$ transition probability of 7.6 ± 1.4 W.u.

III. DISCUSSION

First we note that the isoscalar $(T = 0) \rightarrow (T = 0)$ $B(E2; 3_1^+ \rightarrow 1_1^+)$ value is quite large and certainly not of pure single-particle character. Within the uncertainties it coincides with the $(T = 1) \rightarrow (T = 1)$ $B(E2; 2_2^+ \rightarrow 0_1^+)$ value of 9.1 ± 3.5 W.u. in ^{58}Cu measured earlier by Start *et al.* [18]. The error bar for the $B(E2)$ value between the $T = 0$ states measured here is less than half the error bar for the corresponding $B(E2)$ value between the lowest $T = 1$ states.

We introduce the isoscalar (IS) $E2$ ratio

$$R_{\text{IS}}(J) = \frac{B(E2; J_{T=1}^+ \rightarrow (J - 2)_{T=1}^+)}{B(E2; (J + 1)_{T=0}^+ \rightarrow (J - 1)_{T=0}^+)} \qquad (3)$$

as a convenient indicator for whether isoscalar $E2$ transitions, either between $T = 0$ states or $T = 1$ states, originate from
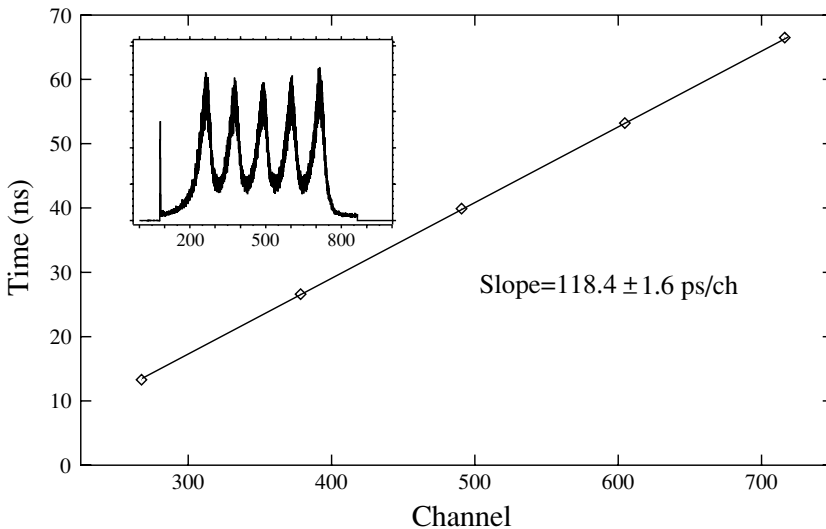

FIG. 4. Time calibration with a calibration spectrum in the inset. The radii of the data points correspond to the statistical errors.

Slope=118.4 ± 1.6 ps/ch

similar structures. If they do, one expects a value $R_{IS}(J) \approx 1$. For ^{58}Cu, the experimental value of $R_{IS}(2)$ is 1.20(51).

In the QDCs picture the $B(E2)$ values for transitions between states with the same isospin quantum number and spins $J + 2$ and J are given by [1,2]

$$B(E2; J + 2 \to J) = \frac{5}{16\pi} \frac{3D(j, J)D(j, J + 1)}{2(2J + 3)(2J + 5)}$$
$$\times (e_p + e_n)^2 \left(\frac{\langle j ||r^2|| j \rangle}{4 j(j + 1)} \right)^2, \quad (4)$$

where $D(j, J) = (2j + 2 + J)(2j - J)(J + 1)$ is a geometrical factor and the radial matrix element $\langle j ||r^2|| j \rangle = A^{1/3}(N + \frac{3}{2})$ fm^2, with N being the principal oscillator quantum number, was calculated from harmonic oscillator radial wave functions. The QDCs ratio $R_{IS}^{QDC}(J)$ is independent of the effective charges and of the radial part and it depends on the geometry of the spin couplings, only. Its value for ^{58}Cu is 1.67, for $J = 2$. This value indicates that both $E2$ transition strengths originate from the same mechanism. However, when considering the absolute $B(E2; 3^+_{T=0} \to 1^+_{T=0})$ value, from Eq. (4), and the experimental value, one obtains a total effective isoscalar $E2$ charge $e_p + e_n = 5.9(5) e$, which is larger than the generally accepted values of effective quadrupole charges $e_p + e_n \approx 2e$ by a factor of about 3. This fact points to a more collective origin of these isoscalar $E2$ transitions and suggests the need to take into account larger configurational spaces.

The next step would be the inclusion of the higher orbitals, $f_{5/2}$ and $p_{1/2}$, of the fp-shell, considering ^{56}Ni as inert core. But, as seen in Ref. [9], this leads to unsatisfactory predictions as compared to experimental results. For example, the $2^+_{T=1} \to 1^+_{T=0}$ isovector $M1$ transition is predicted to be $1.53\mu_N^2$ or $0.82\mu_N^2$ depending on the effective charge taken into consideration, while the experimental value is smaller than $0.011\mu_N^2$. Moreover, the two versions of shell model calculations, Th-2a and Th-2b from Ref. [9], give isoscalar $E2$ ratios of $R_{IS}^{Th-2a}(2) = 17$ and $R_{IS}^{Th-2b}(2) = 15$ in disagreement with the data. Indeed, their $E2$ strengths for the $J^\pi = 2^+_2, T = 1 \to J^\pi = 0^+_1, T = 1$ transition are comparable with the experimental value while the calculated $E2$ strengths for the $J^\pi = 3^+_1, T = 0 \to J^\pi = 1^+_1, T = 0$ transition are smaller than the experimental value by an order of magnitude. This underestimation of the collectivity of the $3^+_1 \to 1^+_1$ $E2$ transition corresponds to an overestimation of the 3^+_1 excitation energy above the 1^+_1 ground state. Th-2 gives the 3^+_1 state at an excitation energy of 980 keV [9], while the measured excitation energy is 444 keV. Parts of the $3^+_1 \to 1^+_1$ $E2$ transition strength are shifted to higher excited 3^+ states in Th-2, e.g., for the calculated $3^+_2, T = 0$ state the isoscalar

TABLE I. Experimental and calculated $B(E2)$ transition probabilities in ^{58}Cu. The large-scale shell-model calculations results were obtained with the GXPF1 interaction.

$B(E2; J^\pi_i \to J^\pi_f)$	Expt. [e^2 fm^4]	LSSM[a], [e^2 fm^4]	$T_i \to T_f$
$B(E2; 3^+_1 \to 1^+_1)$	101(18)	84	$0 \to 0$
$B(E2; 2^+_2 \to 0^+_1)$	122(47)	136	$1 \to 1$
$B(E2; 2^+_2 \to 3^+_1)$	2^{+9}_{-2}	1.5	$1 \to 0$
$B(E2; 2^+_2 \to 1^+_1)$	<60	0.4	$1 \to 0$

[a]Taken from Ref. [9].

$E2$ ratios are $R_{IS}^{Th-2}(2) = 1.03$. Obviously, Th-2 does not describe well the $E2$ collectivity in the $T = 0$ part of the low-spin level scheme of ^{58}Cu and a larger shell model space is more desirable.

Comparisons of predictions of modern large-scale shell-model (LSSM) calculations performed with the new effective GXPF1 interaction [20] which includes core excitations and of small space shell-model calculations that do not include core excitations [21] with experimental data for ^{58}Cu lead to concluding a high degree of softness of the doubly magic $N = Z = 28$ ^{56}Ni nucleus [9]. This translates into an enhanced collectivity which, in turn, implies large $B(E2)$ transition probabilities. The isoscalar $E2$ ratio for the LSSM calculations amounts to $R_{IS}^{LSSM}(2) = 1.62$. This value is in agreement, within experimental uncertainties, with the data. It is close to unity which indicates similar origin for the $\Delta T = 0$ $E2$ strengths between the lowest states with either $T = 0$ or $T = 1$. Agreement between model and data extends now also to absolute $B(E2)$ values. Our measurement, $B(E2; 3^+_1 \to 1^+_1) = 101(18)e^2$ fm^4, is, within error bars, in accord with the theoretical value predicted by the LSSM calculations and therefore confirms its hypothesis. Experimental and theoretical transition strengths are displayed in Table I.

It comes natural to compare the ^{58}Cu data with available data for other nuclei that exhibit a ^{58}Cu-like structure: one proton and one neutron in the same $j = l + 1/2$ orbital outside a closed shell at the $N = Z$ line. Such data are available for ^{18}F and ^{42}Sc and displayed together with the new measurement in Table II. In fact, large isoscalar $E2$ values are not uncommon for $N = Z$ doubly-magic $+ p + n$ nuclei, both between $T = 1$ and between $T = 0$ states. For $T = 1 \to T = 1$ all ^{58}Cu-like nuclei show $B(E2) \approx 10$W.u. while for $T = 0 \to T = 0$ $B(E2) \approx 6$W.u.. The $B(E2)$ values for ^{58}Cu are the largest, possibly indicating the highest softness of the doubly-magic nucleus ^{56}Ni, as compared to ^{16}O and ^{40}Ca, with respect to the coupling of a proton-neutron pair. The experimental isoscalar $E2$ ratios, $R_{IS}(2)$, are compared

TABLE II. Experimental $B(E2)$ transition strengths between quasideuteron states with the same isospin quantum number and experimental and QDC isoscalar $E2$ ratios in ^{58}Cu and ^{58}Cu-like nuclei [24].

Element	$B(E2; 2^+_{T=1} \to 0^+_{T=1})$ W.u.	$B(E2; 3^+_{T=0} \to 1^+_{T=0})$ W.u.	$R_{IS}(2)$	$R_{IS}^{QDC}(2)$
^{18}F	>8	5.8(2)	>1.33	1.0
^{42}Sc	8(3)	4.0(7)	2.0(7)	0.89
^{58}Cu	9.1(35)	7.6(14)	1.20(51)	1.67

with the corresponding predictions of the QDC scheme in Table II. Values of about 1 indicate similar structures in the $T = 0$ and $T = 1$ parts of the spectrum. Numerical shell model calculations [22,23] have been previously performed for ^{18}F and ^{42}Sc using ^{16}O and ^{40}Ca, respectively, as inert cores. While the $B(E2; 3^+_{T=0} \to 1^+_{T=0})$ transition rates for ^{18}F and ^{42}Sc are well reproduced by those calculations, the $B(E2; 2^+_{T=1} \to 0^+_{T=1})$ values come out too weak by a factor of about 2. Kuo and Osnes suggest [23] that this deviation might be caused by neglection of core-deformed components. The present experimental uncertainties in some of the $B(E2)$ values are too large for drawing more definitive conclusions.

The LSSM calculations predict collective $E2$s for the $2^+_2 \to 0^+_1$ and $3^+_1 \to 1^+_1$ transitions. Both are major fractions of Q-phonon excitations on top of the lowest state with $T = 1, 0^+_1$ and the lowest state with $T = 0, 1^+_1$, respectively. Indeed, the 2^+_2 state is the isobaric analog state of the 2^+ Q-phonon excitation in ^{58}Ni. The 3^+_1 state carries approximately 70% of the Q-phonon strength according to the LSSM calculations of Th-1 in Ref. [9]. Actually, the experimental branching ratio for transitions from the 3^+_2 state indicates that the $B(E2; 3^+_2 \to 1^+_1)$ might have been over-predicted in Th-1 which would result in an even higher Q-phonon purity of the 3^+_1 state than already found in the calculation. The 3^+_1 state of ^{58}Cu can be considered as one of the rare cases of a quite pure Q-phonon excitation of the ground state with isospin quantum number $T = 0$.

In summary, we have measured the first $(T = 0) \to (T = 0)$ $E2$ transition rate in the heavy odd-odd N = Z nucleus ^{58}Cu. The lifetime of the $T = 0, 3^+_1$ state of ^{58}Cu at 444 keV was measured to $\tau = 0.468 \pm 0.085$ ns. This level decays by an isoscalar $E2$ transition to the 1^+_1 ground state with a transition strength of $B(E2; 3^+_1 \to 1^+_1) = 7.6 \pm 1.4$ W.u. This $E2$ transition rate is significantly higher than predicted by shell model calculations using configurational spaces restricted to $p_{3/2}$, $f_{5/2}$, and $p_{1/2}$ orbitals, i.e., that consider ^{56}Ni as inert core. On the contrary, the experimental finding agrees within the uncertainties with previous predictions from a LSSM calculation of the Tokyo-group using the GXPF1 interaction and ^{40}Ca as inert core while a considerable amount of excitations from the $f_{7/2}$ shell was predicted. In comparison to other odd-odd N = Z nuclei with one proton and one neutron more than doubly-closed shell core, ^{58}Cu shows the largest isoscalar $E2$ excitation strengths, both in the $(T = 1) \to (T = 1)$ and in the $(T = 0) \to (T = 0)$ cases.

ACKNOWLEDGMENTS

[1] A. F. Lisetskiy, R. V. Jolos, N. Pietralla, and P. von Brentano, Phys. Rev. C **60**, 064310 (1999).

[2] A. F. Lisetskiy, A. Gelberg, R. V. Jolos, N. Pietralla, and P. von Brentano, Phys. Lett. **B512**, 290 (2001).

[3] C. Frießner, N. Pietralla, A. Schmidt, I. Schneider, Y. Utsuno, T. Otsuka, and P. von Brentano, Phys. Rev. C **60**, 011304(R) (1999).

[4] A. Schmidt, I. Schneider, C. Frießner, A. Lisetskiy, N. Pietralla, T. Sebe, T. Otsuka, and P. von Brentano, Phys. Rev. C **62**, 044319 (2000).

[5] I. Schneider, A. F. Lisetskiy, C. Frießner, R. V. Jolos, N. Pietralla, A. Schmidt, D. Weißhaar, and P. von Brentano, Phys. Rev. C **61**, 044312 (2000).

[6] N. Pietralla, R. Krücken, C. J. Barton, C. W. Beausang, M. A. Caprio, R. F. Casten, J. R. Cooper, A. A. Hecht, J. R. Novak, N. V. Zamfir, A. Lisetskiy, and A. Schmidt, Phys. Rev. C **65**, 024317 (2002).

[7] O. Möller, K. Jessen, A. Dewald, A. F. Lisetskiy, P. von Brentano, A. Fitzler, J. Jolie, A. Linnemann, B. Saha, and K. O. Zell, Phys. Rev. C **67**, 011301(R) (2003).

[8] A. F. Lisetskiy, A. Schmidt, I. Schneider, C. Frießner, N. Pietralla, and P. von Brentano, Phys. Rev. Lett. **89**, 012502 (2002).

[9] A. F. Lisetskiy, N. Pietralla, M. Honma, A. Schmidt, I. Schneider, A. Gade, P. von Brentano, T. Otsuka, T. Mizusaki, and B. A. Brown, Phys. Rev. C **68**, 034316 (2003).

[10] G. Siems, U. Neuneyer, I. Wiedenhöver, S. Albers, M. Eschenauer, R. Wirowski, A. Gelberg, P. von Brentano, and T. Otsuka, Phys. Lett. **B320**, 1 (1994).

[11] T. Otsuka and K.-H. Kim, Phys. Rev. C **50**, R1768 (1994).

[12] N. Pietralla, P. von Brentano, R. F. Casten, T. Otsuka, and N. V. Zamfir, Phys. Rev. Lett. **73**, 2962 (1994).

[13] E. A. Phillips and A. D. Jackson, Phys. Rev. **169**, 917 (1968).

[14] P. J. Brussard and P. W. M. Glaudemans, *Shell-Model Applications in Nuclear Spectroscopy* (North-Holland, Amsterdam 1977).

[15] M. Honma, T. Mizusaki, and T. Otsuka, Phys. Rev. Lett. **77**, 3315 (1996).

[16] H. Schatz *et al.*, Phys. Rep. **294**, 167 (1998).

[17] W. Andrejtscheff, M. Senba, N. Tsoupas, Z. Z. Ding, P. Raghavan, Nucl. Instrum. Methods **204**, 123 (1982).

[18] D. F. H. Start, L. E. Carlson, D. A. Hutcheon, A. G. Robertson, E. K. Warburton, and J. J. Weaver, Nucl. Phys. **A193**, 33 (1972).

[19] H. Weisberg and S. Berko, Phys. Rev. **154**, 249 (1967).

[20] M. Honma, T. Otsuka, B. A. Brown, and T. Mizusaki, Phys. Rev. C **65**, 061301(R) (2002).

[21] A. Plastino, R. Arvieu, and S. A. Moszkowski, Phys. Rev. **145**, 837 (1966).

[22] T. T. S. Kuo and E. Osnes, J. Phys. G: Nucl. Phys **6**, 335 (1980).

[23] T. T. S. Kuo and E. Osnes, Phys. Rev. C **12**, 309 (1975).

[24] National Nuclear Data Center, Brookhaven National Laboratory, http://www.nndc.bnl.gov/(2005).